Planetary Candidates from K2 Campaign 16

The Astronomical Journal, 156:22 (18pp), 2018 July https://doi.org/10.3847/1538-3881/aac6e6

Planetary Candidates from *K*2 Campaign 16

Liang Yu[1], Ian J. M. Crossfield[1], Joshua E. Schlieder[2], Molly R. Kosiarek[3,18], Adina D. Feinstein[4], John H. Livingston[5], Andrew W. Howard[6], Björn Benneke[7], Erik A. Petigura[6,19], Makennah Bristow[8], Jessie L. Christiansen[9], David R. Ciardi[9], Justin R. Crepp[10], Courtney D. Dressing[11], Benjamin J. Fulton[7,20], Erica J. Gonzales[3,18], Kevin K. Hardegree-Ullman[12], Thomas Henning[13], Howard Isaacson[11], Sébastien Lépine[14], Arturo O. Martinez[14], Farisa Y. Morales[15,16], and Evan Sinukoff[6,17]

[1] Department of Physics, and Kavli Institute for Astrophysics and Space Research, Massachusetts Institute of Technology, Cambridge, MA 02139, USA
[2] NASA Goddard Space Flight Center, 8800 Greenbelt Road, Greenbelt, MD 20771, USA
[3] Department of Astronomy and Astrophysics, University of California, Santa Cruz, CA 95064, USA
[4] Department of Physics and Astronomy, Tufts University, Medford, MA 02155, USA
[5] Department of Astronomy, Graduate School of Science, The University of Tokyo, Hongo 7-3-1, Bunkyo-ku, Tokyo, 113-0033, Japan
[6] Cahill Center for Astrophysics, California Institute of Technology, Pasadena, CA 91125, USA
[7] Division of Geological and Planetary Sciences, California Institute of Technology, Pasadena, CA 91125, USA
[8] Department of Physics, University of North Carolina at Asheville, Asheville, NC 28804, USA
[9] Caltech/IPAC-NASA Exoplanet Science Institute, 770 S. Wilson Avenue, Pasadena, CA 91106, USA
[10] Department of Physics, University of Notre Dame, Notre Dame, IN 46556, USA
[11] Department of Astronomy, University of California, Berkeley, CA 94720, USA
[12] The University of Toledo, 2801 West Bancroft Street, Mailstop 111, Toledo, OH 43606, USA
[13] Max Planck Institute for Astronomy, Königstuhl 17, D-69117 Heidelberg, Germany
[14] Department of Physics & Astronomy, Georgia State University, 25 Park Place NE #605, Atlanta, GA 30303, USA
[15] Jet Propulsion Laboratory, California Institute of Technology, 4800 Oak Grove Drive, Pasadena, CA 91109, USA
[16] Department of Physical Sciences, Moorpark College, 7075 Campus Road, Moorpark, CA 93021, USA
[17] Institute for Astronomy, University of Hawai'i, Honolulu, HI 96822, USA
Received 2018 March 11; revised 2018 May 14; accepted 2018 May 16; published 2018 June 21

Abstract

Given that Campaign 16 of the *K*2 mission is one of just two *K*2 campaigns observed so far in "forward-facing" mode, which enables immediate follow-up observations from the ground, we present a catalog of interesting targets identified through photometry alone. Our catalog includes 30 high-quality planet candidates (showing no signs of being non-planetary in nature), 48 more ambiguous events that may be either planets or false positives, 164 eclipsing binaries, and 231 other regularly periodic variable sources. We have released light curves for all targets in C16 and have also released system parameters and transit vetting plots for all interesting candidates identified in this paper. Of particular interest is a candidate planet orbiting the bright F dwarf HD 73344 ($V = 6.9$, $K = 5.6$) with an orbital period of 15 days. If confirmed, this object would correspond to a $2.56 \pm 0.18\,R_{\oplus}$ planet and would likely be a favorable target for radial velocity characterization. This paper is intended as a rapid release of planet candidates, eclipsing binaries, and other interesting periodic variables to maximize the scientific yield of this campaign, and as a test run for the upcoming *TESS* mission, whose frequent data releases call for similarly rapid candidate identification and efficient follow up.

Key words: methods: data analysis – planets and satellites: detection – techniques: photometric

1. Introduction

By any measure, NASA's *K*2 mission (Howell et al. 2014) has been a success. Out of the ashes of an ailing spacecraft has risen a tremendously productive scientific mission. Sometime this year, *K*2 will likely run out of the propellant needed to maintain its stable pointing and deliver precise time-series photometry. 2018 is perhaps an appropriate year for this event, as it marks the 40 year anniversary of the first American summit of *K*2—the "Savage Mountain." Hundreds of planets and other astrophysical phenomena have been studied with *K*2, far fewer than the thousands discovered by the original *Kepler* mission (Thompson et al. 2018)—just as thousands of climbers have summited Mount Everest even though only hundreds have ever reached the top of *K*2. Nonetheless, even after the mission ends, an enduring kinship will remain between those who have been fortunate enough to use *K*2 in their research efforts.

In that same communal spirit, we provide a rapid, public release of light curves, planet candidates, and other interesting periodic variables from *K*2's Campaign 16 (C16) in this paper. Unlike most fields observed by *K*2, C16 was observed in "forward-facing" mode, meaning that the field was observable throughout the night as soon as the campaign ended. We have conducted a quick-look analysis of uncalibrated C16 cadence data and are releasing these data products in order to maximize the scientific yield of this campaign. We hope that this will also provide a test for the imminent *TESS* mission, whose frequent data releases will also benefit from rapid candidate identification and follow up.

This paper is organized as follows: In Section 2, we describe how we compute time-series photometry and search for transit-like signals. Section 3 then discusses our approach for discriminating between various astrophysical signals and measurement noise. Finally, in Section 4, we conclude by discussing several particularly interesting systems and reviewing the overall C16 candidate sample.

[18] NSF Graduate Research Fellow.
[19] NASA Hubble Fellow.
[20] Texaco Fellow.

2. *K2* Targets and Photometry

2.1. Target Selection and C16 Data Characteristics

*K*2 target selection is entirely community driven, with all targets selected from Guest Observer (GO) proposals. Our team has proposed large samples of F, G, K, and M dwarfs for every *K*2 Campaign up to Campaign 17, but in the analysis that follows, we use data from all *K*2 GO proposals to maximize the science yield from this campaign.

During C16, *K*2 observed 20647 stars in a field centered at R.A. = 08:54:50, decl. = +18:31:31, for a period of 80 days between 2017 December 07 and 2018 February 25. This is only the second campaign in which the spacecraft was pointed along the forward-facing direction of its velocity vector (the other, C9, was dedicated mostly to microlensing and was in a dense field unsuited for standard transit searches). Forward-facing observations enable simultaneous observations from the ground and with *K*2, and they also allow the field to be accessed from ground-based observatories as soon as compelling targets can be identified. C16 also overlaps with C5 except for a 40-px-wide strip that is not on silicon in C16. We find that 6167 targets observed in C16 were also observed in C5.

2.2. Time-series Photometry

Raw cadence pixel data for C16 became available on the Mikulski Archive for Space Telescopes (MAST)[21] on 2018 February 28. We first convert the raw cadence data into target pixel files with `kadenza`[22] (Barentsen & Cardoso 2018), following the approach described in Christiansen et al. (2018).

From then on, we process the data using a photometric pipeline that has been described in detail in past works by members of our team (e.g., Crossfield et al. 2015; Petigura et al. 2015, 2018). In brief, we follow an approach similar to that originally outlined by Vanderburg & Johnson (2014). We compute the raw photometry by summing the flux within a soft-edged, stationary, circular aperture centered on each target star. During *K*2 operations, solar radiation pressure causes the telescope to roll around its boresight. Consequently, stars trace out small arcs of up to several pixels every ∼6 hr. Interpixel sensitivity variations and aperture losses can then lead to significant changes in the brightness of stars that dominate *K*2 photometry.

To correct for these motion-dependent systematics, we solve for the roll angle between each frame and an arbitrary reference frame using roughly 100 stars of *Kepler* magnitude $Kp \sim 12$ mag on an arbitrary output channel (we typically use channel 4). We then use the publicly available `k2phot` photometry code[23] to model the time- and roll-dependent brightness variations using a Gaussian process with a squared-exponential kernel. The models can be individually applied to the raw photometry to produce photometry corrected for motion-dependent systematics or fully detrended photometry. Figure 1 shows an example of raw *K*2 photometry for a relatively well-behaved star, along with the same light curve after correction for systematics and subsequent detrending. Some light curves with relatively deep transits, as in this example, show small increases in flux immediately before and after the transits. These are artifacts from the detrending process. The transits are effectively outliers on short timescales that may bias the Gaussian process model, leading to overfitting.

We repeat this photometry process for apertures with radii ranging from 1 to 7 pixels, and also fit a custom, automatically generated aperture that selects pixels based on how much flux they receive relative to the background. This aperture has an irregular shape and captures most of the flux from each target. For each target, we adopt the aperture that minimizes the residual noise on 3 hr timescales. Specifically, we use the median absolute deviation (MAD) of the 3 hr Single Event Statistic (SES) as our noise metric. We define the SES as the depth of a box-shaped dimming relative to the local photometric level. This method of aperture selection favors smaller apertures, which incur less background noise, for fainter stars and larger apertures for brighter targets. For strongly saturated stars, the custom aperture is typically chosen, because in these cases circular apertures miss substantial flux.

2.3. Transit Search

We search our calibrated photometry for transit signals using the publicly available `TERRA` algorithm[24] (Petigura et al. 2013a, 2013b). `TERRA` flags targets with putative transits as threshold-crossing events (TCEs), which we later examine visually (see Section 3). Once a TCE is detected, `TERRA` automatically runs again to search for additional signals in the same system (see Petigura et al. 2018) until no more TCEs are found or until the number of candidates exceeds 5.

Many spurious detections at lower S/N are caused by residual outliers in the photometry. In order to reduce the number of spurious detections, we require that TCEs have orbital periods longer than 0.5 days, and that they also show at least three transits. This last criterion rules out any planets with periods longer than half the campaign baseline, or ∼40 days. Thus, many longer-period planets likely remain to be found in this data set. Furthermore, we adopt a threshold of $S/N \geqslant 12$ to yield a good balance between sensitivity to shallow transits and the number of spurious detections. In previous catalog papers produced using the fully processed target pixel files released later by the *K*2 project office, we typically vetted candidates down to a lower S/N threshold of 10. We find that spurious detections are more frequent in light curves derived from uncalibrated cadence data than when using fully calibrated pixel files.

In total, `TERRA` produced a list of 1097 TCEs in C16 with nominal $S/N \geqslant 12$. The distribution of their orbital periods is shown in Figure 2.

3. Triage and Vetting

The majority of TCEs identified by `TERRA` are not caused by genuine transiting planets, but instead by residual instrumental artifacts, eclipsing binary stars, or other periodic stellar variability (e.g., pulsations and spot modulations). We manually vet our entire list of 1097 TCEs to differentiate between these various signals. This process results in a list of robust planet candidates for further follow up and validation, as well as a list of eclipsing binaries and other periodically variable sources.

[21] https://archive.stsci.edu/k2/
[22] https://github.com/KeplerGO/kadenza
[23] https://github.com/petigura/k2phot
[24] https://github.com/petigura/terra

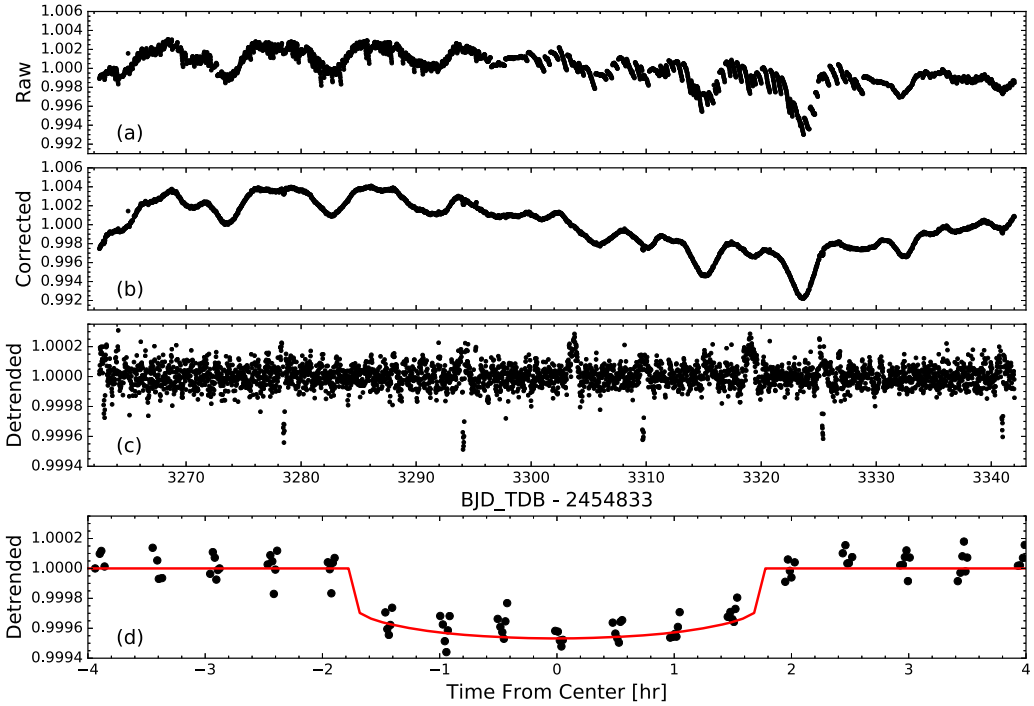

Figure 1. *K*2 photometry of HD 73344 ($V = 6.9$) and its planet candidate, EPIC 212178066.01. From top to bottom: raw aperture photometry; after removal of telescope systematics, revealing a likely 8.5 ± 0.5 day rotation period; after detrending, clearly revealing candidate transits; and after phase-folding and overplotting a model transit profile (red). The bumps in panel (c) do not occur on the same period as the candidate transit and may be artifacts of the detrending process.

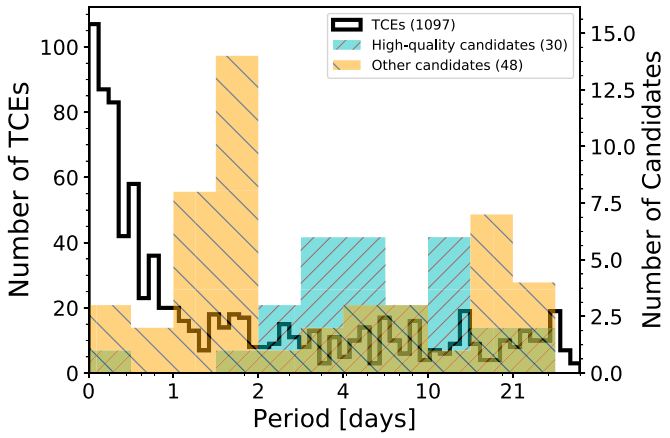

Figure 2. Orbital periods of transit-like signals identified in our analysis. The unfilled, narrow-binned histogram (axis at left) shows the Threshold-crossing Events (TCEs) identified by TERRA in our initial transit search (see Section 2.3). The coarser histograms (axis at right) indicate the distributions of 30 high-quality candidates (blue-green) and 48 remaining, plausibly planetary candidates (orange).

We promote TCEs showing no obvious warning signs to the status of "planet candidate" in the spirit of "*Kepler* Objects of Interest" (KOIs), i.e., events that are almost certainly astrophysical in nature and not obviously false positive scenarios such as eclipsing binaries or variable stars. Details of the vetting process are described in Crossfield et al. (2016) and Petigura et al. (2018). TERRA produces a set of diagnostics for every TCE, which we use to classify the event as a candidate planet, eclipsing binary, periodic variable, or noise. The diagnostics include a summary of basic fit parameters and a suite of diagnostic plots to visualize the nature of the TCE. These plots include the TERRA periodogram, a normalized phase-folded light curve with the best-fit Mandel & Agol (2002) model, the light curve phased to 180° to look for eclipses or misidentified periods, the most probable secondary eclipse identified at any phase, and an autocorrelation function. In the era of *TESS*, cross-matching to ground-based surveys will be another excellent way to discover false positives (e.g., Oelkers et al. 2018).

Table 1 lists the 30 highest-quality planet candidates whose light curves (shown in Figure 3) show no obvious signs of being non-planetary in nature; our experience with four years of *K*2 data leads us to believe that most of these are indeed real planets, ready to be confirmed (e.g., via mass measurements) or statistically validated.

Table 2 lists 48 candidates that could also be transiting planets but include some ambiguous warning signs such as a V-shaped transit (frequently caused by eclipsing binaries). Some candidates in this list may be real planets, but many are likely non-planetary. Following the examples of the KOIs and of Vanderburg et al. (2016), we do not classify candidates with very deep transits as false positives even though transit depths $\gtrsim$5% very likely indicate eclipsing binaries. Candidates with radii larger than 1.5 R_J were also included in this category, as giant planet candidates from *Kepler* have a false positive rate as high as 50% (Santerne et al. 2016). We plot the light curves of these candidates in Figure 4.

Finally, we identify a larger sample of periodic astrophysical signals that are almost certainly not caused by planets. Table 3 lists 164 targets that clearly show both transits and secondary eclipses, while Table 4 lists the 231 other periodic, astrophysical signals such as pulsations, coherent stellar rotations, and objects identified as galaxies or quasars in the Ecliptic Plane Input Catalog (EPIC; Huber et al. 2016) or GO proposals. There is likely overlap between these last two tables, e.g., for short-period contact/near-contact binaries whose light curves may have been classified as periodic variables.

Table 1
High-quality candidate parameters

Candidate	*Kp*	*P* [d]	T_0 [BJD - 2454833]	T_{14} [d]	$(R_P/R_*)^2$ [ppm]	R_*[a] [$R_\odot$]	M_*[a] [$M_\odot$]	$T_{\rm eff}$[a] [K]	log g[a] [cgs]	R_P [$R_\oplus$]	$S_{\rm inc}$ [$F_\oplus$]	In C5?	Comment
211502222.01	11.617	22.995920	3280.30425	0.155	470	1.043 ± 0.015	1.054 ± 0.060	6010 ± 170	4.426 ± 0.031	2.5	49		—
211529065.01	13.431	4.399871	3264.73662	0.0532	1076	0.772 ± 0.006	0.852 ± 0.019	4810 ± 30	4.594 ± 0.010	2.8	115	yes	—
211533633.01	13.258	2.126953	3262.66212	0.059	707	0.573 ± 0.018	0.585 ± 0.024	4020 ± 220	4.696 ± 0.015	1.7	105		—
211552050.01	13.194	3.544965	3264.95164	0.061	621	0.701 ± 0.007	0.718 ± 0.037	4860 ± 120	4.602 ± 0.024	1.9	149		—
211631538.01	14.221	5.513327	3266.24778	0.0386	2119	0.770 ± 0.014	0.791 ± 0.046	5020 ± 110	4.562 ± 0.030	3.9	105		—
211638401.01	14.763	0.530270	3262.64176	0.0443	568	0.558 ± 0.006	0.578 ± 0.013	3880 ± 70	4.706 ± 0.011	1.4	553		—
211647930.01	11.982	14.759595	3264.39324	0.1712	1705	1.186 ± 0.024	1.068 ± 0.079	6070 ± 190	4.318 ± 0.043	5.3	118		—
211673349.01	14.446	4.894289	3264.62726	0.0877	3043	0.686 ± 0.008	0.712 ± 0.026	4440 ± 50	4.620 ± 0.018	4.1	64		—
211730024.01	11.402	5.113823	3263.81018	0.0896	1054	1.409 ± 0.036	1.356 ± 0.084	6890 ± 340	4.274 ± 0.041	5.0	968		—
211741619.01	13.564	2.787663	3263.82026	0.0311	1087	0.602 ± 0.005	0.627 ± 0.016	3950 ± 30	4.676 ± 0.013	2.2	71		—
211812935.01[b]	12.64	3.607981	3264.87890	0.1141	5543	2.253 ± 0.081	1.573 ± 0.085	6490 ± 210	3.928 ± 0.042	18.3	2815		—
211816003.01	13.654	14.454034	3265.79062	0.114	1374	0.802 ± 0.012	0.824 ± 0.056	5490 ± 80	4.548 ± 0.036	3.2	44	yes	—
211919004.01	13.131	11.722103	3265.36820	0.1546	958	0.838 ± 0.008	0.920 ± 0.027	5170 ± 60	4.556 ± 0.015	2.8	46	yes	—
211945201.01	10.115	19.491965	3280.94047	0.124	1777	1.485 ± 0.357	1.335 ± 0.183	6320 ± 300	4.219 ± 0.152	6.8	129	yes	—
212036875.01	10.937	5.169887	3265.67929	0.0646	3348	1.450 ± 0.036	1.380 ± 0.084	6830 ± 390	4.256 ± 0.041	9.1	970		—
212040382.01	12.521	4.445559	3266.34866	0.1513	4228	2.237 ± 0.082	1.565 ± 0.082	6520 ± 270	3.932 ± 0.038	15.9	2150		—
212041476.01	12.078	2.783705	3262.55831	0.053	538	0.939 ± 0.013	0.985 ± 0.046	5890 ± 150	4.487 ± 0.025	2.4	643		—
212058012.01	11.018	11.561514	3266.10708	0.1281	255	1.406 ± 0.315	1.305 ± 0.147	6140 ± 220	4.255 ± 0.146	2.4	211		—
212069861.01	14.102	30.954222	3274.10848	0.1368	1496	0.598 ± 0.007	0.609 ± 0.016	4040 ± 80	4.671 ± 0.013	2.5	3	yes	K2-123 b [Dressing et al. 2017]
212072539.01	14.874	7.676984	3263.56938	0.0733	2124	0.465 ± 0.010	0.488 ± 0.014	3790 ± 80	4.790 ± 0.011	2.3	11	yes	—
212081533.01	12.731	3.355854	3262.74687	0.0635	670	0.551 ± 0.005	0.579 ± 0.013	3860 ± 10	4.720 ± 0.011	1.6	45		—
212099230.01	10.513	7.112134	3269.13703	0.1046	553	1.042 ± 0.151	1.016 ± 0.109	5800 ± 250	4.409 ± 0.092	2.7	208	yes	—
212110888.01	11.441	2.995653	3263.95700	0.0813	8175	1.398 ± 0.032	1.235 ± 0.095	6380 ± 270	4.239 ± 0.045	13.8	1521	yes	K2-34 b [Lillo-Box et al. 2016, Hirano et al. 2016]
212154564.01	15.105	6.414008	3264.81383	0.0699	4614	0.394 ± 0.010	0.413 ± 0.012	3620 ± 80	4.863 ± 0.014	2.9	9	yes	K2-124 b [Dressing et al. 2017]
212178066.01	6.793	15.613426	3262.89291	0.1256	362	1.438 ± 0.218	1.378 ± 0.155	6460 ± 220	4.264 ± 0.090	3.0	175		HD 73344
212204403.01	12.482	4.688625	3263.71310	0.0964	1777	0.828 ± 0.010	0.875 ± 0.043	5220 ± 100	4.545 ± 0.029	3.8	166		possible multi
212204403.02	12.482	12.550896	3271.42819	0.1179	858	0.828 ± 0.010	0.875 ± 0.043	5220 ± 100	4.545 ± 0.029	2.6	44		possible multi
212219881.01	15.147	6.924808	3264.18479	0.1189	9578	0.795 ± 0.027	0.817 ± 0.055	5300 ± 70	4.550 ± 0.037	8.5	101		—
251319382.01[c]	11.116	8.236486	3265.71419	0.1293	401	0.923 ± 0.014	0.973 ± 0.046	5930 ± 120	4.497 ± 0.024	2.0	151		possible multi
251319382.02[c]	11.116	14.869943	3270.60950	0.1193	1900	0.923 ± 0.014	0.973 ± 0.046	5930 ± 120	4.497 ± 0.024	4.4	67		possible multi

Notes.
[a] Note that all uncertainties reported in this table and Table 2 are statistical uncertainties only and do not account for systematic uncertainties in the underlying stellar models.
[b] Parameters not in EPIC; classified using `isochrones` as described in Section 1.
[c] Possible multi, but the ephemeris of 251319382.01 matches that of another TCE (see Table 2). We identified hints of a third candidate in this system, with a period of ∼3.5 day and S/N∼7.

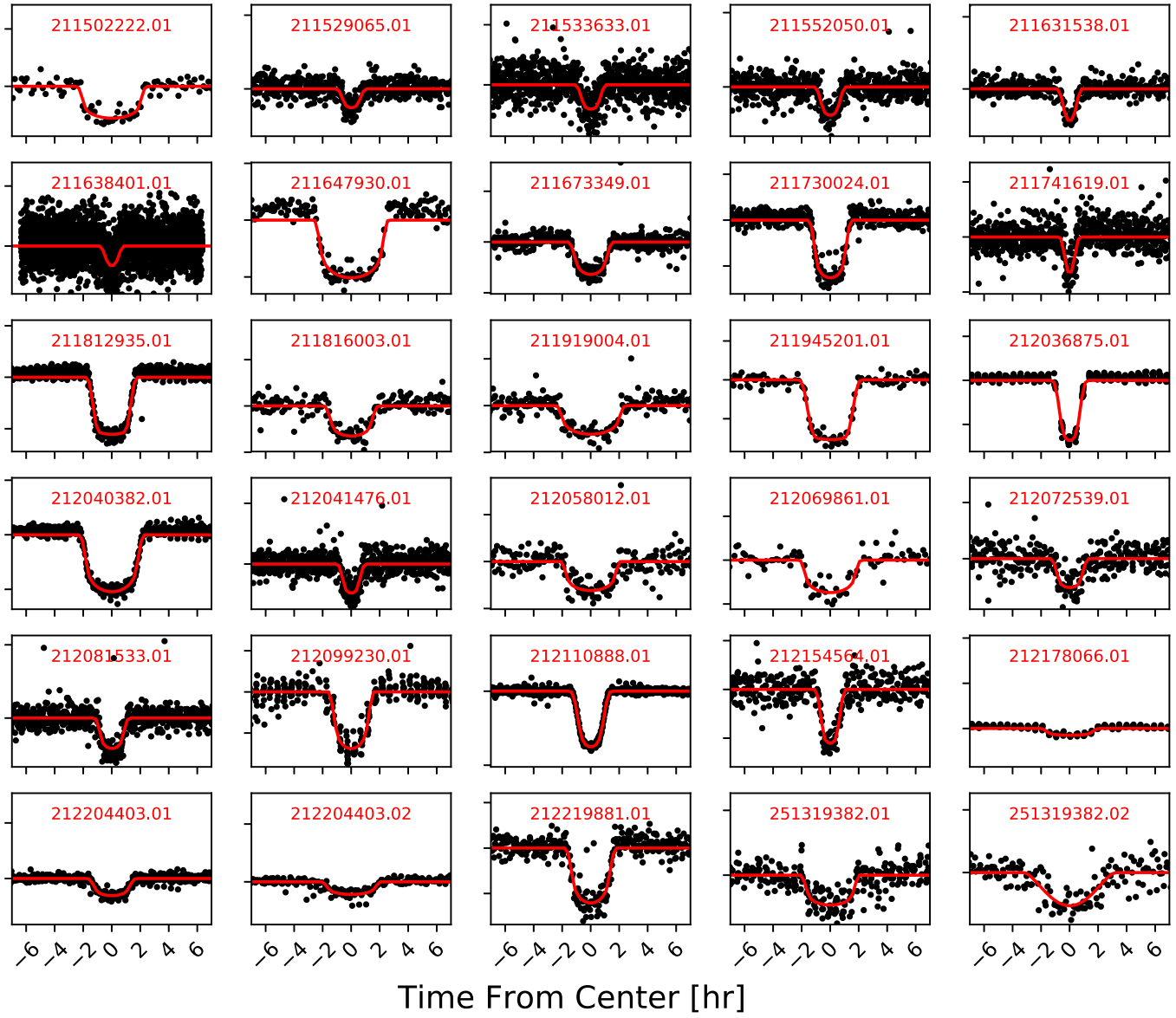

Figure 3. Phase-folded light curves of our 30 high-quality planet candidates, and their best-fit Mandel & Agol (2002) transit models. To avoid clutter, we did not label the *y*-axis. Their system parameters are listed in Table 1.

After constructing the samples of astrophysical TCEs described above, we also perform ephemeris matching following the approach of Coughlin et al. (2014). By adopting their recommended thresholds for periods and times-of-transit, we identify a number of transit-like signals with matching ephemerides. We do not discard any of these systems but indicate them in our target tables. This matching exercise also led us to demote three systems that we had originally classified as high-quality candidates (211914445.01, 211964332.01, and 251319382.01) down into a lower tier.

To provide the community access to these candidates as rapidly as possible, we have chosen to forego a full MCMC analysis on each candidate's light curve. Instead, we run a Levenberg–Marquardt minimization on each planet candidate to fit a Mandel & Agol (2002) transit model. The stellar limb-darkening parameters are fixed to values derived using the `PyLDTk` package[25] (Parviainen & Aigrain 2015) and stellar parameters derived in Section 4.1. We find that this fit gives us a more reliable estimate of the transit ephemerides than `TERRA`. For periodic variables and systems with secondary eclipses, we merely report the parameters found by `TERRA`. In some cases, `TERRA` obviously identified a multiple of the true period, and we include a note to that effect where appropriate.

[25] https://github.com/hpparvi/ldtk/tree/v1.0

4. Discussion

4.1. Host Star Parameters

Unlike the original *Kepler* mission, *K*2 does not have a homogeneous catalog of stellar parameters. Fortunately, we still have the benefit of the comprehensive classification catalog of *K*2 targets produced by Huber et al. (2016), who used mainly a combination of colors and galactic population synthesis models to derive stellar parameters such as effective temperatures ($T_{\rm eff}$), surface gravities ($\log g$), metallicities ([Fe/H]), radii, masses, densities, distances, and extinctions for *K*2 stars. The typical precision of these classifications is

Table 2
Plausible candidate parameters

Candidate	*Kp*	*P* [d]	T_0 [BJD - 2454833]	T_{14} [d]	$(R_P/R_*)^2$ [ppm]	R_* [$R_\odot$]	M_* [$M_\odot$]	$T_{\rm eff}$ [K]	log *g* [cgs]	In C5?	Comment	Ephemeris matching
211397844.01	13.292	16.168833	3274.81174	0.1331	4046	5.653 ± 0.284	2.750 ± 0.454	5186 ± 135	3.371 ± 0.090			
211492384.01	12.375	0.635328	3262.97422	0.0543	1315	1.531 ± 0.047	1.286 ± 0.096	6420 ± 300	4.176 ± 0.050		somewhat V-shaped	
211503824.01	11.246	2.047195	3263.17910	0.0789	255	0.958 ± 0.013	1.000 ± 0.046	6150 ± 110	4.476 ± 0.023		slightly asymmetric	
211543616.01	15.6	1.518232	3263.37623	0.1284	356389	1.209 ± 0.074	0.914 ± 0.073	5510 ± 210	4.237 ± 0.062		V-shaped	
211544257.01	12.242	1.630130	3263.45081	0.0952	46964	1.602 ± 0.047	1.286 ± 0.082	6190 ± 230	4.136 ± 0.041		somewhat V-shaped; spotted star?	
211546613.01	15.982	2.007472	3263.89429	0.0377	16989	0.473 ± 0.012	0.495 ± 0.016	3790 ± 70	4.783 ± 0.013		V-shaped	
211611139.01[a]	12.474	1.882213	3263.60257	0.0402	5678	1.568 ± 0.140	1.355 ± 0.106	6590 ± 380	4.178 ± 0.081		somewhat V-shaped	
211616939.01	11.796	1.855400	3262.61930	0.1167	775	10.091 ± 0.531	3.490 ± 0.558	4990 ± 140	2.964 ± 0.070		V-shaped	211619805.01, 211620138.01, 211663688.01
211619805.01	12.942	1.855827	3262.60966	0.1257	844	0.664 ± 0.010	0.684 ± 0.030	4720 ± 140	4.627 ± 0.021		somewhat V-shaped	211616939.01, 211620138.01, 211663688.01
211620138.01	9.512	1.855421	3262.61863	0.2368	660084	2.734 ± 0.224	3.081 ± 0.529	11500 ± 1960	4.055 ± 0.141		V-shaped	211616939.01, 211619805.01, 211663688.01
211642882.01	13.788	23.897707	3267.90399	0.0618	11511	0.728 ± 0.009	0.738 ± 0.040	5020 ± 120	4.581 ± 0.027		V-shaped	
211649214.01	14.726	3.787950	3265.41821	0.0688	4851	4.182 ± 0.153	1.896 ± 0.435	5126 ± 136	3.476 ± 0.117			
211663688.01	16.419	1.855516	3262.61467	0.1698	14554	0.189 ± 0.010	0.161 ± 0.008	3110 ± 110	5.092 ± 0.026		V-shaped	211616939.01, 211619805.01, 211620138.01
211733267.01	12.15	8.657975	3264.32036	0.041	6106	0.891 ± 0.016	0.819 ± 0.060	5370 ± 140	4.450 ± 0.041	yes	slightly V-shaped	
211814313.01	15.431	15.405101	3265.30794	0.1172	16796	1.475 ± 0.142	1.112 ± 0.099	5910 ± 210	4.145 ± 0.076		V-shaped	
211830293.01	11.916	20.893526	3281.64853	0.3209	8821	1.765 ± 0.045	1.249 ± 0.085	6020 ± 260	4.041 ± 0.042		possible eclipse at phase 0.53	
211863149.01	14.873	2.612990	3264.30341	0.2776	2779	0.458 ± 0.004	0.480 ± 0.009	3520 ± 20	4.798 ± 0.009		V-shaped	211839430.01, 211839462.01
211876245.01	15.518	8.971460	3266.46199	0.1086	269917	0.872 ± 0.037	0.840 ± 0.063	5330 ± 150	4.481 ± 0.050		Somewhat V-shaped; hint of eclipse	
211886472.01	11.126	19.639750	3281.74841	0.0591	4477	2.183 ± 0.124	1.599 ± 0.096	6730 ± 370	3.963 ± 0.052	yes	V-shaped	
211892395.01	16.238	0.995061	3262.63670	0.1102	445224	0.864 ± 0.039	0.801 ± 0.037	5080 ± 140	4.468 ± 0.038		V-shaped	
211914445.01	14.529	1.810718	3263.47161	0.1002	1366	1.178 ± 0.043	0.914 ± 0.072	5680 ± 200	4.257 ± 0.050	yes	—	211914889.01, 211914960.01, 211915147.01
211914889.01	18.032	1.810420	3263.48113	0.1544	35275	0.313 ± 0.013	0.230 ± 0.070	3050 ± 20	4.808 ± 0.201	yes	somewhat V-shaped	211914445.01, 211914960.01, 211915147.01
211914960.01	14.179	1.810834	3263.46871	0.1185	3433	0.888 ± 0.205	0.241 ± 0.253	3230 ± 690	3.921 ± 0.581	yes	V-shaped	211914445.01, 211914889.01, 211915147.01
211946007.01	16.57	1.982809	3263.84986	0.0568	213762	0.291 ± 0.020	0.281 ± 0.019	3330 ± 160	4.958 ± 0.035	yes	Transiting brown dwarf AD 3116 [Gillen et al. 2017]	
211964332.01	14.533	7.220537	3266.50370	0.1714	3983	0.932 ± 0.035	0.865 ± 0.072	5420 ± 160	4.435 ± 0.053			211964001.01, 211964025.01, 211964555.01, 251809628.01
211969807.01	15.149	1.974991	3262.86291	0.0705	1310	0.484 ± 0.012	0.504 ± 0.016	3820 ± 70	4.773 ± 0.013	yes	K2-104 b [Mann et al. 2017]; marginal detection.	
211972627.01	11.353	1.092845	3263.45807	0.0677	236	0.951 ± 0.013	0.968 ± 0.058	5620 ± 70	4.468 ± 0.032	yes	V-shaped	211972681.01, 211972837.01
211972681.01	15.39	1.092673	3263.46283	0.0544	833	0.783 ± 0.025	0.807 ± 0.050	5140 ± 160	4.557 ± 0.035		V-shaped (or short transit duration)	211972627.01, 211972837.01
211997641.01	12.821	1.744546	3263.51613	0.1635	206372	2.316 ± 0.133	1.636 ± 0.091	6530 ± 350	3.921 ± 0.049	yes	v-shaped	
212024672.01	18.174	3.697161	3262.87327	0.1397	35827	0.245 ± 0.013	0.216 ± 0.054	3120 ± 20	4.991 ± 0.109	yes	slightly V-shaped; hint of eclipse	212024647.01
212033577.01	11.835	23.702342	3285.09327	0.226	48619	1.869 ± 0.048	1.334 ± 0.076	6280 ± 190	4.021 ± 0.037		V-shaped	
212041206.01	14.671	23.917716	3283.38421	0.0717	32061	0.828 ± 0.019	0.803 ± 0.048	5050 ± 110	4.507 ± 0.033		V-shaped	
212048748.01	12.771	5.745912	3262.55671	0.0472	3155	0.307 ± 0.003	0.302 ± 0.007	3390 ± 20	4.943 ± 0.010		V-shaped	
212052250.01	14.743	0.986765	3262.87581	0.139	305455	1.400 ± 0.067	1.141 ± 0.085	6080 ± 230	4.201 ± 0.050		V-shaped –likely even-odd	
212068493.01	12.955	14.220246	3271.79491	0.1452	101983	1.461 ± 0.045	1.200 ± 0.102	6130 ± 270	4.185 ± 0.050		V-shaped	

Table 2
(Continued)

Candidate	Kp	P [d]	T_0 [BJD - 2454833]	T_{14} [d]	$(R_P/R_*)^2$ [ppm]	R_* [$R_\odot$]	M_* [$M_\odot$]	$T_{\rm eff}$ [K]	$\log g$ [cgs]	In C5?	Comment	Ephemeris matching
212096658.01	10.21	1.466473	3263.68144	0.1062	335755	0.981 ± 0.016	0.911 ± 0.029	4570 ± 110	4.413 ± 0.023	yes	V-shaped	
212114260.01	12.311	20.016917	3265.54619	0.1006	5520	0.970 ± 0.019	0.972 ± 0.066	5790 ± 130	4.451 ± 0.037		likely eclipse	
212159514.01	13.704	0.545702	3262.55728	0.0798	532	4.752 ± 0.307	2.707 ± 0.292	5330 ± 170	3.514 ± 0.071	yes	somewhat asymmetric	
212194007.01	12.824	1.177150	3262.94420	0.1635	294749	2.529 ± 0.105	1.639 ± 0.077	6390 ± 200	3.846 ± 0.036		V-shaped	
212207368.01	15.626	1.190316	3263.29198	0.1358	14098	0.335 ± 0.027	0.338 ± 0.021	3420 ± 200	4.916 ± 0.043		V-shaped	212223307.01
212223307.01	10.962	1.190354	3263.29164	0.1635	363154	2.407 ± 0.048	1.611 ± 0.080	6350 ± 180	3.880 ± 0.030		V-shaped	212207368.01
212227092.01	16.226	5.190254	3266.42803	0.1317	696741	0.645 ± 0.012	0.139 ± 0.006	3120 ± 10	3.970 ± 0.020		V-shaped	
212228994.01	13.553	1.095841	3263.34496	0.0796	3489	1.906 ± 0.050	1.309 ± 0.062	5920 ± 130	3.996 ± 0.030		V-shaped; variable depth	
251279430.01	9.438	0.719597	3262.56479	0.0639	149	1.224 ± 0.016	1.184 ± 0.071	6080 ± 130	4.338 ± 0.033		somewhat V-shaped	
251288417.01	15.991	20.924593	3279.57804	0.0639	119088	0.423 ± 0.004	0.103 ± 0.004	2980 ± 10	4.198 ± 0.018		V-shaped	
251292838.01	12.157	19.581519	3274.28569	0.1132	85946	0.861 ± 0.015	0.900 ± 0.051	5638 ± 121	4.525 ± 0.029			
251294036.01	13.636	6.854931	3268.73159	0.0526	11053	1.031 ± 0.018	0.854 ± 0.051	5360 ± 130	4.343 ± 0.036		somewhat V-shaped	
251380988.01	12.434	30.921004	3274.20687	0.2285	169142	1.761 ± 0.079	1.425 ± 0.102	6680 ± 380	4.099 ± 0.053		slightly V-shaped	

[a] Parameters not in EPIC; classified using `isochrones` as described in Section 1.

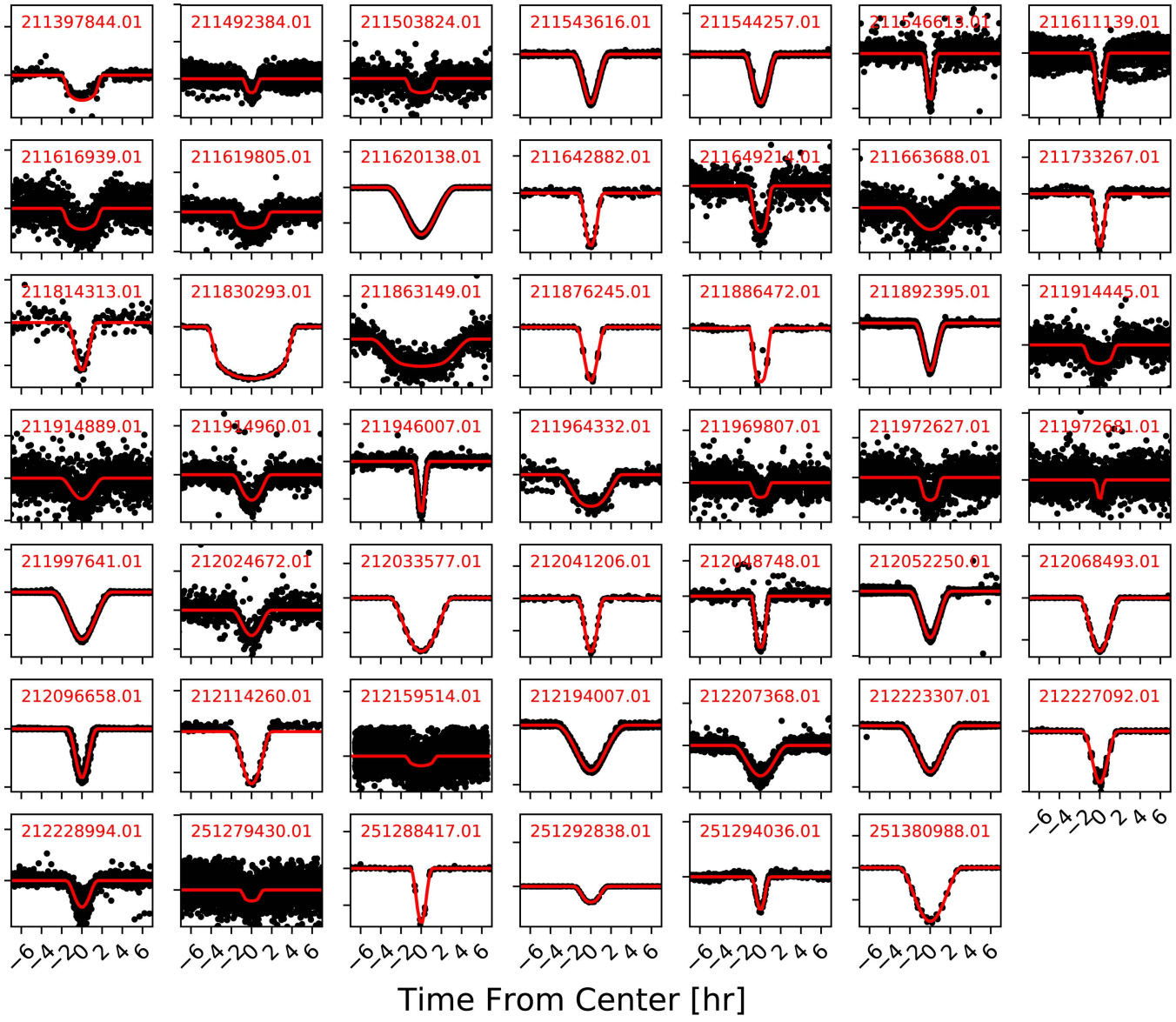

Figure 4. Phase-folded light curves of our 48 lower-quality planet candidates, and their best-fit Mandel & Agol (2002) transit models. Typical transit depths for these candidates range from 300 to 700,000 ppm. Their system parameters are listed in Table 2.

≈2%–3% in $T_{\rm eff}$ (Huber et al. 2016). However, the Huber et al. (2016) analysis misclassifies 55%–70% of subgiants as dwarfs and relies on Padova stellar models (Marigo et al. 2008), which systematically underestimate the stellar radii of M dwarfs by up to 20%. Many C16 targets, including all of our planet candidate hosts, also have parallaxes from *Gaia* DR2 (Gaia Collaboration et al. 2016, 2018). We used the parallaxes and the `isochrones` package[26] (Morton 2015) in conjunction with the broadband photometry (*BVJHKgri*) from the EPIC to infer the $T_{\rm eff}$, stellar radii, $\log g$, [Fe/H] and masses of all planet candidate hosts. In Tables 1 and 2, we list the median stellar parameters and their 1σ uncertainties from `isochrones` for all of our candidates. For the vast majority of the candidates, the best-fit $T_{\rm eff}$ is consistent with that from Huber et al. (2016) at the 2σ level. But we note that the reported uncertainties are only statistical uncertainties and do not account for any systematic uncertainties in the underlying stellar models, and may therefore be underestimated, especially for cooler stars.

Figure 5 shows the Huber et al. (2016) $T_{\rm eff}$ (where available) for the entire C16 sample, along with the `isochrones`-derived $T_{\rm eff}$ distribution among our planet candidate samples. The full campaign shows three distinct populations of targets observed by *K*2, with peaks around 3500, 5000, and 6100 K. The number of candidates is of course much lower, but the distribution of $T_{\rm eff}$ for these systems appears to roughly track that of the underlying target distribution even though we do not expect it to, given the change in planet detectability as a function of stellar magnitude, radius, and noise.

4.2. Characteristics of the Planet Candidate Sample

The period distribution of our planet candidates, along with that of the TCEs, is shown in Figure 2. Whereas the TCE distribution peaks for $P < 1$ day, the number of high-quality candidates increases toward longer periods as expected for real planets (e.g., Morton et al. 2016; Fulton et al. 2017). A larger

[26] https://github.com/timothydmorton/isochrones

Table 3
Systems with Secondary Eclipses

Candidate	*Kp*	*P* [d]	T_0 [BJD_{TDB} - 2454833]	T_{14} [d]	$(R_P/R_*)^2$ [ppm]	In C5?	Comment	Ephemeris matching
211397774.01	15.649	0.967865	3262.83095	0.1047	149235		even-odd –half-period	
211402878.01	14.498	25.236580	3277.84155	0.1427	131088			
211408138.01	12.740	10.337864	3267.82296	0.2954	50598	yes		
211409299.01	11.951	13.919301	3263.16370	0.2036	126507	yes		
211411891.01	12.776	0.954863	3262.53608	0.0928	122533			
211422822.01	15.664	0.554633	3262.67870	0.0547	26770			
211425822.01	14.888	2.153178	3263.18086	0.1114	161675			
211429934.01	14.147	0.565934	3262.47647	0.0817	76907			
211430148.01	14.892	15.091257	3262.98697	0.1731	387212	yes		
211431013.01	14.738	3.102398	3265.15784	0.2575	116056	yes	even-odd –half-period	
211432167.01	8.550	5.817737	3263.03384	0.1202	9442	yes		211432176.01
211432176.01	9.866	5.817854	3263.03296	0.1200	9632			211432167.01
211432946.01	14.398	1.671965	3263.07264	0.0897	321572	yes	even-odd –half-period	
211449931.01	14.659	6.663685	3262.53719	0.1092	77241			
211452175.01	12.406	11.114394	3268.75989	0.2596	140535			
211453076.01	16.341	0.524461	3262.66075	0.0714	8800		twice period	
211453223.01	14.590	9.056947	3264.66347	0.1389	228283			
211468153.01	14.381	0.737735	3262.69611	0.0817	293171			
211471048.01	12.867	0.799768	3262.64738	0.1499	368062			
211477347.01	15.368	1.641114	3263.39459	0.1835	232835			
211490299.01	15.991	0.555516	3262.88867	0.0616	125677			
211492541.01	12.789	1.031746	3262.80400	0.2313	13062			
211493669.01	12.976	0.583370	3262.72350	0.0485	16936			
211509665.01	16.519	3.247194	3263.55605	0.1960	274993		even-odd –half-period	
211524114.01	11.473	0.715676	3262.65638	0.0520	1668			
211524558.01	14.161	0.546969	3262.99346	0.0817	496880	yes	twice period	
211526186.01	12.814	0.682618	3262.60560	0.0487	10943	yes	even-odd –1.5× period	
211534342.01	15.873	0.512702	3262.52406	0.0751	259506			
211535481.01	14.979	0.539696	3262.52362	0.0727	101331		V-shaped; likely even-odd	
211538193.01	13.908	0.597258	3262.98601	0.0817	250566			
211540348.01	14.022	0.620388	3262.73962	0.0817	497678			
211563123.01	12.583	17.325857	3265.30498	0.3548	334820	yes		
211589784.01	12.678	1.359386	3263.68715	0.0767	92013	yes		
211600389.01	14.157	0.630717	3263.02647	0.0817	163414			211600632.01
211600632.01	16.688	0.630718	3263.02663	0.0817	164032			211600389.01
211604981.01	12.727	12.427163	3267.32649	0.2241	16631			
211607670.01	12.793	1.348851	3263.01356	0.1584	217820		even-odd –half-period	
211607804.01	13.358	1.490219	3263.43270	0.1635	733825			
211613886.01	12.729	0.958786	3263.10671	0.0522	17691	yes		
211619120.01	13.059	11.100314	3264.29172	0.5242	123582	yes		
211621644.01	15.443	0.921358	3262.74784	0.0694	127918		thrice period	
211621961.01	16.548	11.078847	3265.06284	0.5970	121654			
211625003.01	12.848	0.530431	3262.92711	0.0817	409431		even-odd; 1.5× period	
211626490.01	12.886	0.747734	3262.90935	0.0817	287143			
211630537.01	14.185	0.697190	3262.80305	0.0773	34039			
211631904.01	13.989	0.884004	3262.66371	0.0882	391961	yes		
211638883.01	12.622	0.543877	3262.47515	0.0282	659			
211639283.01	15.088	6.741846	3266.59522	0.3020	55296		slightly V-shaped	
211644647.01	13.304	2.044175	3264.21457	0.2978	71960		even-odd –half-period	
211651743.01	13.962	0.516235	3262.68635	0.0817	111574			
211662047.01	14.791	0.635238	3262.94146	0.0637	126462			
211663508.01	14.343	0.544418	3262.51405	0.0813	434869		four times period	
211664543.01	15.812	0.698333	3262.97188	0.0550	106429		thrice period	
211710534.01	12.203	3.022569	3263.74324	0.1410	56458			
211718105.01	14.103	2.958763	3264.20177	0.2411	176980		even-odd –half-period	
211721325.01	15.428	1.052364	3262.72164	0.1179	348537			
211732801.01	10.655	2.131554	3263.40544	0.1694	68562	yes	V-shaped; even-odd –half-period	251411166.01
211737652.01	16.354	2.468190	3262.93777	0.2452	483890			
211738534.01	15.604	0.568020	3262.64187	0.1389	13803			
211744153.01	14.861	4.612166	3265.94990	0.0664	5543	yes		
211750072.01	13.005	0.595558	3263.09743	0.0705	51711			

Table 3
(Continued)

Candidate	*Kp*	*P* [d]	T_0 [BJD_{TDB} - 2454833]	T_{14} [d]	$(R_P/R_*)^2$ [ppm]	In C5?	Comment	Ephemeris matching
211759163.01	14.804	0.595667	3262.90859	0.0620	129607		five times period	
211764271.01	12.895	3.576744	3262.91264	0.1222	68508			211764373.01
211764373.01	11.409	3.576780	3262.91248	0.1111	31467		likely SE	211764271.01
211768007.01	14.021	0.542912	3262.56186	0.0748	120270		twice period	
211770390.01	12.239	3.790180	3262.68640	0.2469	52183	yes	even-odd –half-period	
211807456.01	14.973	0.504961	3262.86244	0.0756	291504		twice period	
211809568.01	15.456	0.593274	3262.99164	0.0817	636988		twice period	
211812160.01	13.485	1.085097	3262.91626	0.0898	31653	yes		
211814733.01	11.971	14.707213	3268.97802	0.0892	4206	yes		
211822953.01	16.834	1.549381	3262.83336	0.0684	92689	yes		
211828142.01	17.558	20.180269	3268.57729	0.1192	395334			
211829982.01	13.823	5.803439	3264.34997	0.1628	627831			
211838158.01	15.801	0.575349	3262.87166	0.0817	522455		twice period	
211839430.01	10.730	2.612938	3264.30391	0.3813	114984	yes	even-odd –half-period	211863149.01, 211839462.01
211839462.01	10.037	2.612804	3264.30654	0.3681	91385	yes	even-odd –half-period	211863149.01, 211839430.01
211841496.01	15.486	0.522199	3262.46826	0.0676	35912			
211852187.01	17.636	14.343042	3266.06818	0.0610	110696			
211858408.01	12.427	0.628876	3262.79149	0.0817	109867			
211858489.01	12.270	0.636109	3262.49271	0.0290	1465			
211885185.01	12.493	4.397187	3262.92467	0.2452	203447	yes		
211906940.01	16.368	0.526316	3262.47776	0.0418	364733	yes	thrice period	
211910237.01	14.750	1.108972	3263.36936	0.0760	37369	yes	odd-even –half-period	
211914718.01	11.448	0.582017	3262.66714	0.0817	376942	yes	twice period	
211915147.01	9.023	1.810708	3263.47340	0.1267	35675	yes	odd-even; half-period	211914445.01, 211914889.01, 211914960.01
211919555.01	16.889	9.484994	3264.50601	0.6098	82338			211920528.01, 211920604.01, 251809286.01
211919842.01	15.625	9.510911	3264.32358	0.4087	7834			
211920462.01	19.874	9.516793	3264.29495	0.4087	408803			
211920528.01	12.279	9.486580	3264.50407	0.4341	2153	yes		211919555.01, 211920604.01, 251809286.01
211920604.01	12.258	9.487929	3264.49219	0.5031	8783	yes		211919555.01, 211920528.01, 251809286.01
211920811.01	12.482	9.492590	3264.47004	0.4525	4713	yes		
211928959.01	16.703	0.858462	3263.16644	0.0845	248568			
211934173.01	18.229	0.520451	3262.60163	0.0259	34196	yes		
211942157.01	12.051	1.324292	3263.37798	0.2452	249317	yes		
211955798.01	14.902	0.616444	3263.06087	0.0290	5674		thrice period	
211964001.01	9.402	7.218071	3266.51847	0.1993	32035			211964332.01, 211964025.01, 211964555.01, 251809628.01
211964025.01	7.605	7.219626	3266.50648	0.2035	31796			211964332.01, 211964001.01, 211964555.01, 251809628.01
211964555.01	18.314	7.220943	3266.50089	0.2204	34667			211964332.01, 211964001.01, 211964025.01, 251809628.01
211972837.01	13.547	1.092917	3263.45491	0.1566	1355446	yes		211972627.01, 211972681.01
212009702.01	13.173	0.923861	3263.37075	0.1382	345965	yes		
212010565.01	14.531	2.851451	3263.72690	0.3877	992969			
212012387.01	13.972	3.244126	3264.32148	0.1609	405896	yes	even-odd –half-period	
212019055.01	12.700	0.821436	3263.14571	0.0991	162008	yes		
212020442.01	13.974	3.888853	3263.60805	0.1295	25872	yes	even-odd –half-period	
212024647.01	10.279	3.696871	3262.87322	0.1286	124336	yes		212024672.01
212026226.01	16.843	1.769505	3263.39804	0.1512	176962		even-odd –half-period	
212037403.01	13.231	3.408190	3265.44045	0.1191	164327	yes		
212039539.01	11.647	2.229820	3263.61073	0.2225	247831			
212044495.01	12.733	1.830767	3263.40493	0.1187	157032			
212048503.01	13.625	0.617674	3262.65639	0.0817	598171		twice period	
212053988.01	15.028	0.579309	3262.53528	0.0817	471689		twice period	
212060710.01	14.273	1.204338	3262.76086	0.1057	406463			
212060895.01	16.782	0.604228	3262.94672	0.0704	196260		twice period	
212066805.01	10.410	0.816734	3262.60536	0.0505	5075			
212069706.01	14.410	0.547674	3262.88638	0.0239	1629	yes	twice-period	
212071939.01	13.598	1.743013	3262.49990	0.2452	470271			

Table 3
(Continued)

Candidate	*Kp*	*P* [d]	T_0 [BJD_{TDB} - 2454833]	T_{14} [d]	$(R_P/R_*)^2$ [ppm]	In C5?	Comment	Ephemeris matching
212075294.01	15.873	0.550820	3262.88533	0.0789	319979		twice period	
212075842.01	14.516	1.153456	3262.92758	0.2072	128377		possible even-odd	
212082682.01	14.611	3.797473	3262.81109	0.1082	118402	yes		
212083250.01	11.967	0.518748	3262.97005	0.0817	157737	yes		212083455.01
212083455.01	12.262	0.518754	3262.96851	0.0344	228	yes		212083250.01
212085654.01	13.900	0.989720	3262.87427	0.1128	168919			
212085740.01	13.688	4.845561	3263.15766	0.1162	77469	yes		
212086717.01	14.757	0.643142	3263.04961	0.0817	450377		twice period	
212109233.01	12.624	1.991357	3262.74598	0.1259	96349			
212110007.01	14.245	16.709659	3264.12649	0.1373	112830	yes		
212115388.01	14.605	1.488249	3262.99356	0.0756	48367		even-odd –half-period	
212116340.01	12.079	0.610205	3262.87662	0.0817	136330	yes		
212117087.01	12.245	1.076390	3262.97882	0.1212	91275		even-odd –half-period	
212154158.01	12.300	1.023613	3263.35564	0.2126	11010			
212163353.01	13.539	5.173531	3265.85411	0.1336	58580	yes		
212171851.01	14.143	5.489456	3266.59388	0.5965	370025	yes		
212175087.01	13.431	0.699705	3262.85587	0.1975	244959			
212181307.01	15.502	0.555317	3262.74524	0.0817	416594		twice period	
212181460.01	14.620	0.569192	3262.70026	0.0817	276502			
212182233.01	14.991	0.751394	3262.93405	0.0817	628169			
212207194.01	12.285	9.148701	3265.32727	0.2275	119700			
212208163.01	15.437	2.724469	3263.01388	0.2452	665629			
212210390.01	13.136	12.886147	3262.90925	0.1161	62814			
212214592.01	13.803	0.723102	3263.08482	0.0820	58108			
212221986.01	15.093	0.526018	3262.72081	0.0597	236909			
212225413.01	13.937	0.793048	3263.13909	0.1360	200400			
212225806.01	15.251	0.594392	3262.90962	0.0817	406214		double period	
212225986.01	13.668	1.160308	3263.03616	0.0993	205206		even-odd –half-period	
212228588.01	14.794	0.598120	3262.85185	0.0606	108294			251307609.01
228682364.01	19.970	0.872893	3263.15278	0.1432	68394	yes		
251281013.01	14.183	3.287912	3265.59014	0.1247	107725		even-odd –half-period	
251286992.01	15.448	0.505602	3262.78219	0.0740	410848		twice period	
251292508.01	15.238	1.288312	3263.63014	0.0829	241729		even-odd –half-period	
251307609.01	15.183	0.598197	3262.86830	0.0817	379663		twice period	212228588.01
251308775.01	11.989	2.804246	3263.72840	0.1635	69100			
251314585.01	14.440	0.691617	3263.02339	0.0817	98244			
251315031.01	13.537	0.540527	3262.97430	0.0788	333734			
251327548.01	11.636	11.349445	3268.62400	0.2443	59759			
251330444.01	11.202	5.998652	3265.28349	0.4500	83190		odd-even –half-period.	
251345848.01	12.505	2.883162	3263.26254	0.1305	37899			
251345849.01	16.059	0.545251	3262.96562	0.0817	139220			
251347050.01	12.290	0.493967	3262.55539	0.0895	17723			
251353301.01	14.556	0.504475	3262.67601	0.0772	87373			
251356484.01	14.484	0.781949	3262.81038	0.1084	186838			
251356953.01	14.568	5.214590	3266.48141	0.1706	555674			
251383916.01	16.220	1.332797	3263.21492	0.1635	645357			
251390801.01	13.319	0.592255	3262.47910	0.0817	312313		twice period	
251393748.01	11.256	8.071810	3266.66297	0.1346	190291			
251393916.01	15.093	0.678473	3262.53788	0.0755	58984			
251394139.01	11.763	26.286249	3277.27748	0.3626	110497			
251404897.01	16.029	0.660085	3262.70281	0.0817	273793			
251411166.01	14.179	3.374330	3262.71953	0.2550	23276			
251809286.01	16.200	9.485826	3264.49974	0.6392	52542			211919555.01, 211920528.01, 211920604.01
251809628.01	20.140	7.220585	3266.50127	0.2244	38587			211964332.01, 211964001.01, 211964025.01, 211964555.01

fraction of lower-quality candidates have $P < 2$ days; based on the occurrence rates of short-period planets, we expect that many of these shortest-period candidates are not planets.

Figure 6 shows the brightness in the *Kepler* bandpass (*Kp*) and transit depths for our candidates. The highest-quality candidates typically orbit stars with $Kp = 10$–15 mag and have

Table 4
Systems showing periodic variability

Candidate	*Kp*	*P* [d]	In C5?	Comment	Ephemeris matching
211404813.01	16.261	0.560055			
211405917.01	16.664	0.53736	yes		
211417284.01	14.388	0.912345			
211419593.01	14.084	0.544223			
211422471.01	9.95	1.694853			
211432103.01	10.249	0.933482	yes	likely even-odd	
211432905.01	17.747	0.565384	yes		
211433054.01	13.798	0.61983	yes		
211434930.01	14.249	0.619451			
211440296.01	15.179	0.494049		thrice period	
211441441.01	16.838	0.591286			
211442676.01	11.446	0.608446			
211443853.01	14.141	0.561341			
211446249.01	14.273	0.615748		four times period	
211446443.01	16.105	0.592558			212033577.01
211448564.01	14.193	0.601654			
211460030.01	14.43	0.645333			
211460061.01	19.164	0.625954			
211461914.01	14.825	0.65416			
211463443.01	12.52	0.616079			211880558.01
211466875.01	11.368	0.652342			
211467499.01	12.702	0.656892			
211469982.01	16.85	0.610206			
211476633.01	14.316	0.593171			
211478023.01	9.328	0.624181	yes	four times period	
211484212.01	16.047	0.560321	yes		
211489039.01	11.76	0.63247	yes		
211490515.01	14.366	1.028101	yes		
211493788.01	15.443	0.505653			
211497766.01	15.273	0.599943			
211500156.01	14.979	0.512656			
211505322.01	14.512	0.636194			
211505333.01	14.727	0.57382			
211513796.01	14.574	0.497528			211892395.01
211514420.01	14.713	0.625234		thrice period	
211515715.01	13.759	0.656366		four times period	
211523002.01	15.759	0.534137			
211532642.01	17.637	0.6961		thrice period	
211536560.01	16.958	0.549796			
211538914.01	10.11	0.49353	yes		
211548601.01	14.234	0.612276			
211557076.01	13.619	0.75719			
211558647.01	13.173	0.643227		twice period	
211600632.01	16.688	0.630718		galaxy	211600389.01
211604764.01	15.381	0.631078	yes	double period	
211620946.01	13.789	0.510214		thrice period	
211626641.01	16.243	0.53009			
211630761.01	12.248	0.866331			
211635890.01	14.755	0.725634			
211637025.01	15.064	0.730568			
211637624.01	13.35	0.870809			
211638042.01	15.258	0.549654		thrice period	
211638623.01	15.882	0.930924			
211647067.01	15.508	0.588719		four times period	
211648739.01	11.346	0.543899			
211655464.01	14.846	0.536933			
211660114.01	15.758	0.571957			
211661302.01	14.459	0.729855			
211661627.01	14.265	0.567284		four times period	
211663508.01	14.343	0.544418		four times period	
211663804.01	11.477	0.504537		marginal. twice period	
211665162.01	14.071	0.509189			
211675538.01	10.902	0.942686			
211675809.01	16.992	0.576179		four times period	

Table 4
(Continued)

Candidate	*Kp*	*P* [d]	In C5?	Comment	Ephemeris matching
211690514.01	14.863	0.543476		twice period	
211690710.01	10.74	0.546275			
211712111.01	14.052	0.578952			
211719362.01	10.481	0.603347	yes	thrice period	
211723397.01	16.886	0.495563		galaxy	211723536.01
211723536.01	13.946	0.495561			211723397.01
211727340.01	16.741	1.201041			
211731135.01	15.656	0.622298	yes		
211740165.01	12.557	0.506108			
211746225.01	19.166	2.131503		quasar	211732801.01
211761392.01	15.241	0.651541		period multiple	
211763285.01	13.092	0.504204			
211767109.01	14.05	0.602632			
211796365.01	16.387	0.559817			
211812650.01	14.449	0.743778	yes		
211814391.01	15.578	0.514631			
211817361.01	13.595	0.595522	yes		
211821331.01	14.997	0.667574	yes	twice period	
211821355.01	19.48	0.522619	yes		
211836630.01	16.206	0.6466			
211845034.01	16.466	1.332803	yes		
211849962.01	14.307	0.546683			
211856772.01	16.732	0.50999		twice period	
211859760.01	16.567	0.50096			
211862434.01	15.915	0.547386			
211863022.01	14.428	0.805189			
211864337.01	16.056	0.496984			
211869527.01	15.525	1.026173			
211871191.01	16.659	0.558281			
211876205.01	17.528	0.601344			
211880558.01	18.228	0.616146			211463443.01
211881456.01	17.431	0.588505			
211894518.01	12.214	1.288034	yes		
211902331.01	9.332	1.03411			211431013.01
211907820.01	16.895	1.646612			
211909322.01	15.311	0.838731	yes	twice period	
211911525.01	12.114	0.597831			
211914343.01	17.21	1.810841		galaxy	211914445.01, 211914889.01, 211914960.01, 211915147.01
211917859.01	17.481	0.574261		galaxy	
211918335.01	10.042	0.574317	yes		
211918516.01	14.408	0.724075			
211918830.01	12.798	0.692784	yes		
211919555.01	16.889	9.484994		galaxy	211920528.01, 211920604.01, 251809286.01, 251809286.01
211920462.01	19.874	9.516793		quasar	
211921309.01	17.026	9.478705		noisy –possibly variable depth. Galaxy	
211926098.01	13.349	0.509329			
211926877.01	18.414	0.571362	yes		
211927125.01	11.2	0.680888	yes		
211931604.01	11.827	0.828348	yes	twice period	
211938003.01	15.133	0.630256	yes		
211945144.01	13.94	0.65699	yes	twice period	
211945831.01	14.875	0.516025	yes		
211946241.01	14.332	1.189492	yes		
211947405.01	13.973	0.604689	yes		
211948134.01	18.646	0.501662		galaxy	
211950298.01	16.326	0.510436	yes		
211951418.01	15.433	0.564096			
211957146.01	12.603	0.532536	yes		
211957745.01	16.262	0.507392			
211966619.01	15.166	0.800628			
211973080.01	16.339	1.092902		galaxy	211972627.01, 211972681.01, 211972837.01
211996682.01	12.593	1.36468	yes		

Table 4
(Continued)

Candidate	*Kp*	*P* [d]	In C5?	Comment	Ephemeris matching
212001688.01	14.116	0.79668	yes		
212005402.01	15.052	0.679429			
212008305.01	13.037	0.615002	yes		
212011476.01	12.743	0.715915	yes		
212013694.01	15.313	0.552221			
212018921.01	14.748	0.519797	yes		212018980.01
212018980.01	17.863	0.519707			212018921.01
212019712.01	14.115	0.952995	yes		
212021237.01	18.791	0.681632		quasar	212043122.01, 212050004.01
212022582.01	15.127	0.834426			
212024898.01	15.509	0.599922			
212027377.01	17.643	1.106476	yes		
212027952.01	11.29	0.949276			
212028041.01	14.321	0.729797	yes	twice period	
212032754.01	15.853	0.558059			
212037558.01	11.882	0.627062	yes		
212041051.01	16.235	0.627561		four times period	
212043122.01	9.899	0.681463			212021237.01, 212050004.01
212048412.01	14.391	0.502575			
212050004.01	16.496	0.681455		twice period	212021237.01, 212043122.01
212050890.01	13.589	0.966599			
212054062.01	16.709	0.944882			
212055545.01	15.058	0.613025			
212060713.01	15.626	0.61537			
212066299.01	11.324	2.609746			
212085240.01	15.164	0.565691			
212086317.01	14.301	0.535092			
212086389.01	16.282	0.493336		thrice period	
212089888.01	15.346	0.681236			
212091210.01	14.526	0.683492			
212091834.01	16.122	0.908531			
212095395.01	10.106	0.640683	yes		
212102092.01	14.613	1.227465			
212105446.01	14.448	0.586443			
212106797.01	15.529	0.614616		twice period	
212109327.01	12.477	0.492292			
212110857.01	17.75	0.922879	yes		
212114705.01	19.689	0.610284		twice period; quasar	212116340.01
212118200.01	15.204	0.508903			251391268.01
212118344.01	10.719	0.752885			
212159519.01	12.779	0.717385	yes	twice period	
212159586.01	14.621	0.563176			
212161144.01	13.822	0.723318			
212161874.01	16.807	0.572131			
212163652.01	13.465	0.551515			
212164476.01	14.499	0.67844	yes	twice period	
212172621.01	11.764	0.911485	yes		
212174388.01	14.638	0.665443	yes	twice period	
212174434.01	13.481	0.552321		thrice period	
212177756.01	15.782	0.491506			
212180386.01	17.422	0.718264		double period	
212183082.01	17.322	0.575069			
212194110.01	12.819	0.520576			212194171.01
212194171.01	12.819	0.520576			212194110.01
212199005.01	14.449	0.688457			
212204655.01	15.164	0.709082		likely half-period	
212212241.01	15.624	0.618142			
212222875.01	18.097	1.19013		galaxy	212207368.01, 212223307.01, 212231252.01
212226872.01	16.14	0.516574			
212230240.01	11.887	0.559411			
212231252.01	17.747	1.190356		V-shaped, coincides with 212222875, galaxy	212207368.01, 212223307.01, 212222875.01
251277092.01	12.067	0.502406			
251277701.01	16.014	0.701132			
251278670.01	11.026	0.634153			

Table 4
(Continued)

Candidate	*Kp*	*P* [d]	In C5?	Comment	Ephemeris matching
251279786.01	16.624	0.503283			
251282021.01	16.24	0.527674			
251283448.01	14.032	0.516848			
251283585.01	15.29	0.497466			
251284270.01	13.642	0.688028			
251284826.01	13.557	0.534658			
251290111.01	16.013	0.515451			
251297292.01	14.451	0.521537		thrice period	
251307454.01	16.142	0.551316			211631538.01
251316666.01	14.396	0.567813			
251321168.01	14.203	0.606779			
251321696.01	15.703	0.631561			
251323035.01	14.221	0.596242		thrice period	
251330643.01	19.247	5.997937		quasar	251330444.01
251336933.01	12.952	1.166224			
251342381.01	15.777	0.878144			
251347997.01	14.102	0.497745			
251348935.01	12.852	0.562005			
251349510.01	12.286	0.605516			
251350556.01	16.267	0.699118			
251351108.01	14.098	0.732705			
251355465.01	16.019	0.574342			
251356578.01	11.493	0.788145			
251365170.01	13.313	0.902363			251365173.01
251365173.01	13.563	0.902431		twice period	251365170.01
251374534.01	13.993	0.890305			
251384067.01	17.67	0.527066			
251390658.01	15.332	0.716276			
251391268.01	13.759	0.508759		thrice period	212118200.01
251392383.01	16.699	0.567376			
251397356.01	15.266	1.170258			
251397429.01	12.393	0.542076			
251400494.01	12.922	0.715199		twice period	
251401983.01	14.39	0.836151		twice period	
251402361.01	15.0	0.809957			
251403257.01	16.493	0.638882			
251403570.01	14.633	1.036362			
251809170.01	18.41	0.553061		twice period	
251809263.01	18.93	0.650882			
251809286.01	16.2	9.485826		galaxy	211919555.01, 211920528.01, 211920604.01, 211919555.01
251809628.01	20.14	7.220585		galaxy	211964332.01, 211964001.01, 211964025.01, 211964555.01

transit depths $\gtrsim$100 ppm, as is typical for *K*2 planet catalogs (e.g., Mayo et al. 2018). One candidate has $Kp = 6.8$ mag and is a clear outlier; this would be the brightest host star, by far, for any transiting planet discovered by *K*2. We discuss this candidate, HD 73344, in greater detail in Section 4.3 below.

Adopting the stellar parameters derived in Section 4.1, Figure 7 plots the planet radii and incident irradiation of all our candidates.

We detect one possible multi-planet system, with two high-quality candidates around EPIC 212204403. These have periods of 4.7 and 12.6 days and sizes of approximately 3.3 and 2.6 $R_\oplus$, respectively. Based on past studies of multi-planet systems, these candidates are likely to be real planets (Lissauer et al. 2012; Sinukoff et al. 2016). Validating them is beyond the scope of this work, but at $V = 12.6$ mag, the system could be an interesting target for radial velocity (RV) mass measurements of multi-planet systems.

Another interesting candidate is EPIC 212048748.01 from the lower-quality "plausible planet candidate" list. This candidate transits with a 3155 ppm depth and a period of 5.75 days around a high proper motion, infrared bright ($K = 9.2$) star having optical-IR photometry consistent with an M3 spectral type. If confirmed, this $\sim$2 $R_\oplus$ candidate will be a priority target for upcoming IR sensitive precision RV instruments and transit spectroscopy with the *James Webb Space Telescope*.

Finally, a comparison with the NASA Exoplanet Archive shows that four of our candidates have already been validated using data from C5. Dressing et al. (2017) validated two of our high-quality C16 candidates, 212069861.01 (K2-123b) and 212154564.01 (K2-124b); another candidate 212110888.01 is a previously known hot Jupiter K2-34b (Hirano et al. 2016; Lillo-Box et al. 2016); and our lower-priority candidate 211969807.01 was validated as K2-104b (Mann et al. 2017).

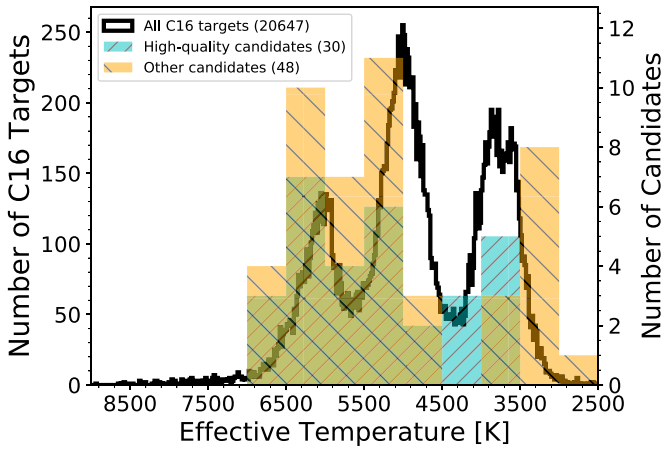

Figure 5. Distribution of EPIC stellar $T_{\rm eff}$ for the entire C16 target sample (empty, fine-grained histogram) and for our planet candidate sample (filled, coarser histograms).

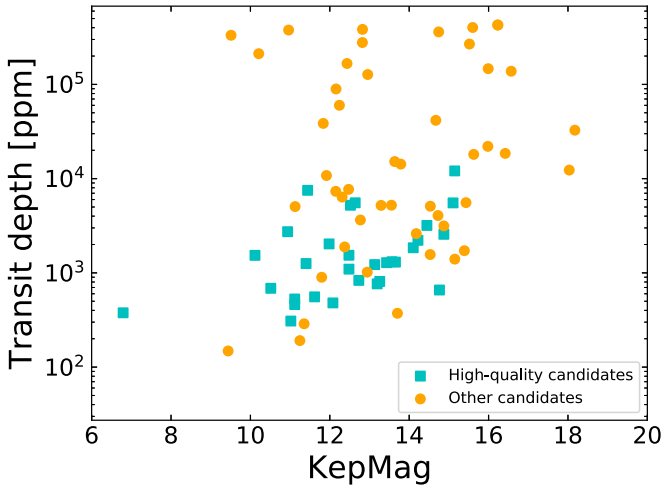

Figure 6. Transit depth and stellar magnitude for our high-quality candidates (light blue squares) and lower-quality candidates (orange circles).

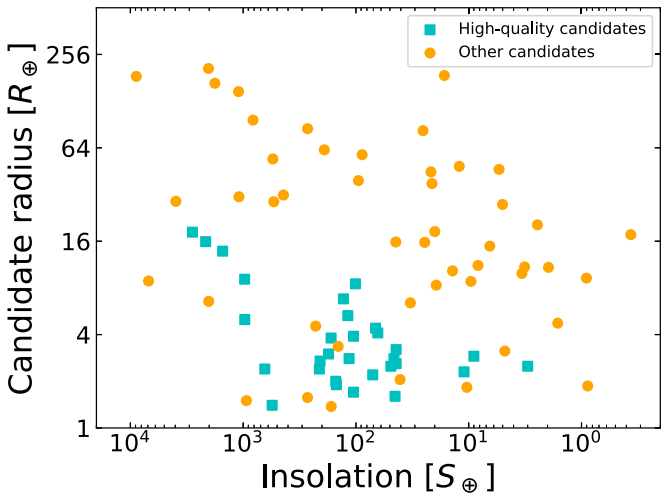

Figure 7. Approximate radii and incident insolation for our high-quality candidates (light blue squares) and lower-quality candidates (orange circles).

Table 5
Candidate Parameters for HD 73344

Parameter	Units	Value
T_0	$\mathrm{BJD_{TDB}}$-2454833	$3262.8931^{+0.0020}_{-0.0023}$
P	day	$15.61335^{+0.00085}_{-0.00078}$
i	deg	$89.15^{+0.61}_{-1.13}$
$R_{\rm circ}/R_*$	%	$2.65^{+0.15}_{-0.10}$
T_{14}	hr	$3.46^{+0.20}_{-0.17}$
T_{23}	hr	$3.22^{+0.21}_{-0.18}$
R_*/a	⋯	$0.0327^{+0.0118}_{-0.0042}$
b	⋯	0.46 ± 0.32
$\rho_{*,\rm circ}$	g cm^{-3}	$2.2^{+1.1}_{-1.3}$
a	au	$0.1321^{+0.0063}_{-0.0070}$
$R_{\rm cand}$	R_E	2.56 ± 0.18
$S_{\rm inc}$	S_E	111^{+12}_{-11}

One more low-quality candidate, 211946007.01, was confirmed to be a transiting brown dwarf (Gillen et al. 2017). Our derived system parameters are in approximate agreement with those in the discovery papers. A combined analysis of the C5 and C16 data (possible for many targets in C16) may prove fruitful for these systems.

4.3. HD 73344

One candidate of particular interest is HD 73344[27] (HIP 42403, EPIC 212178066), and we show the light curve in Figure 1. This bright F star ($V = 6.9$ mag) is highly saturated in the *K*2 data, but a custom aperture encompassing the entire saturated PSF shows the clear transit-like signal highlighted in Figure 1. Because the candidate is exceptionally bright, and thus amenable to future characterization, we investigated the signal more closely than others, as explained below.

The star has been characterized by many groups over the years (e.g., Valenti & Fischer 2005; Paletou et al. 2015). It lies at a distance of 35.296 ± 0.052 pc (Gaia Collaboration et al. 2018) and its parameters are $T_{\rm eff} = 6120 \pm 50$ K, $R_* = 1.15 \pm 0.04\,R_\odot$, $M_* = 1.26 \pm 0.19\,M_\odot$ (Valenti & Fischer 2005), in good agreement with our derived values from *Gaia* DR2 and `isochrones`. The star's projected rotational velocity is $v \sin i = 6.3 \pm 0.5$ km s^{-1} (Valenti & Fischer 2005), and our light curve shows evidence of stellar rotation at a period (determined via Lomb–Scargle periodogram) of 8.5 ± 0.5 days. This period would be consistent with the rotation periods of other stars with similar colors and is consistent with a stellar age of roughly 1 Gyr (Angus et al. 2015). Combining all of these parameters indicates that the stellar rotation axis is inclined by $i = 62° \pm 10°$. Thus, if the candidate signal comes from an object orbiting HD 73344, the angular momentum of the star and the transiting object's orbit are likely misaligned.

Because the star is strongly saturated, we cannot apply a standard centroid analysis of the stellar position in- versus out-of-transit. However, a transit analysis with MCMC (identical to that described by Crossfield et al. 2015) implies a stellar density of $\rho_{*,\rm circ} = 2.2 \pm 1.2$ g cm^{-3}—a loose constraint, but consistent with the spectroscopically inferred stellar density of 1.2 ± 0.2 g cm^{-3} and much higher than the low stellar

[27] This target was proposed by many *K*2 GO programs: 16009 (PI Charbonneau), 16010 (PI Lund), 16021 (PI Howard), 16028 (PI Cochran), 16063 (PI Redfield), 16068 (PI Jensen), and 16081 (PI Guzik).

densities that might be expected from an eclipsed giant star. The results of our transit analysis, which includes dilution as a free parameter, are also consistent with no dilution.

The resulting parameters from our transit analysis of HD 73344 are listed in Table 5. If the transits are occurring around the target and not around a background star in the photometric aperture, the stellar radius and transit depth imply a candidate radius of roughly 2.6 $R_\oplus$. This size would imply a corresponding candidate mass of $10 \pm 3\,M_\oplus$ (Wolfgang et al. 2016) and an RV amplitude of $\sim$2 m s^{-1}. The star was observed 24 times over 11 years as part of the Lick RV survey (Fischer et al. 2014), but these data have an rms of 32 m s^{-1} (despite internal uncertainties of roughly 6 m s^{-1}) and show no coherent RV signal at the candidate period or at our calculated stellar rotation period. Nightly Keck/HIRES RVs over four consecutive nights in 1999 showed a stellar jitter of 3.9 m s^{-1} (Isaacson & Fischer 2010). HD 73344 also exhibits moderate chromospheric activity ($S_{\rm HK} = 0.22$, $R'_{\rm HK} = -4.66$; Isaacson & Fischer 2010), but at this $T_{\rm eff}$ H&K activity is not the main contribution to jitter. It seems likely that precise RV measurements could confirm this planet candidate, despite the fact that it orbits an early-type star, which makes RV measurements more challenging than for later-type stars.

4.4. Conclusions

In a short timespan, we have converted cadence-level *K*2 data into time-series photometry of 20647 targets, identified 1097 periodic signals (of astrophysical or instrumental origin), and distilled these into 30 high-quality planet candidates, 48 lower-quality candidates, 164 eclipsing binaries, and 231 other periodically variable astrophysical sources. Four of our candidates have already been validated as planets (see Section 4.2), suggesting that our approach successfully identifies planet-like signals. One particularly interesting new target is HD 73344, a $V = 6.9$ F dwarf, which may host a 2.6 $R_\oplus$ planet on a 15-day orbit (see Section 4.3). We have released parameters for all identified systems of interest, along with light curves and transit vetting plots.[28] We hope that rapid identification and public dissemination of interesting signals will maximize the scientific productivity of *K*2. If *K*2 continues operating through the end of C17 (another forward-facing campaign), it may prove useful to perform a similarly rapid analysis of those data.

This rapid-release model is also somewhat of an analog for the upcoming *TESS* mission (Ricker et al. 2014). The release of planet catalogs has occurred only irregularly during the *K*2 mission, but this paradigm will change once *TESS* operations begin in earnest. Data from *TESS* will be released and processed on a 27-day rhythm for most of the two-year mission duration. With the shorter observing windows, ephemeris decay is also a much larger problem for *TESS*, and therefore the importance of securing planet candidates in the same season is even higher. If interesting objects could be rapidly gleaned from *TESS* data and circulated to the community, follow-up observations and analyses could begin a full season earlier and so the full impact of that mission could more quickly be achieved.

We thank the anonymous referee and Trevor David for providing helpful comments on the manuscript, and all those who selected the targets observed in C16. I.J.M.C. acknowledges support from NASA through K2GO grant 80NSSC18K0308 and from NSF through grant AST-1824644. He also gratefully acknowledges the hospitality of the organizers and participants of the "Challenge to Super-Earths" workshop at NAOJ, during which much of this work took place. This work made use of the gaia-kepler.fun crossmatch database created by Megan Bedell. This paper includes data collected by the *Kepler* mission. Funding for the *Kepler* mission is provided by the NASA Science Mission directorate. Some of the data presented in this paper were obtained from the Mikulski Archive for Space Telescopes (MAST). STScI is operated by the Association of Universities for Research in Astronomy, Inc., under NASA contract NAS5-26555. Support for MAST for non-*HST* data is provided by the NASA Office of Space Science via grant NNX13AC07G and by other grants and contracts. This research has made use of the Exoplanet Follow-up Observing Program (ExoFOP), which is operated by the California Institute of Technology, under contract with the National Aeronautics and Space Administration.

Facilities: Kepler, *K*2.

[28] All available now at https://exofop.ipac.caltech.edu/k2/, or by request.

ORCID iDs

Liang Yu https://orcid.org/0000-0003-1667-5427
Molly R. Kosiarek https://orcid.org/0000-0002-6115-4359
John H. Livingston https://orcid.org/0000-0002-4881-3620
Andrew W. Howard https://orcid.org/0000-0001-8638-0320
Erik A. Petigura https://orcid.org/0000-0003-0967-2893
Jessie L. Christiansen https://orcid.org/0000-0002-8035-4778
Justin R. Crepp https://orcid.org/0000-0003-0800-0593
Courtney D. Dressing https://orcid.org/0000-0001-8189-0233
Benjamin J. Fulton https://orcid.org/0000-0003-3504-5316
Howard Isaacson https://orcid.org/0000-0002-0531-1073
Arturo O. Martinez https://orcid.org/0000-0002-3311-4085
Farisa Y. Morales https://orcid.org/0000-0001-9414-3851
Evan Sinukoff https://orcid.org/0000-0002-5658-0601

References

Angus, R., Aigrain, S., Foreman-Mackey, D., & McQuillan, A. 2015, MNRAS, 450, 1787
Barentsen, G., & Cardoso, J. V. d. M. 2018, Kadenza: Kepler/K2 Raw Cadence Data Reader, Astrophysics Source Code Library, ascl:1803.005
Christiansen, J. L., Crossfield, I. J. M., Barentsen, G., et al. 2018, AJ, 155, 57
Coughlin, J. L., Thompson, S. E., Bryson, S. T., et al. 2014, AJ, 147, 119
Crossfield, I. J. M., Ciardi, D. R., Petigura, E. A., et al. 2016, ApJS, 226, 7
Crossfield, I. J. M., Petigura, E., Schlieder, J. E., et al. 2015, ApJ, 804, 10
Dressing, C. D., Vanderburg, A., Schlieder, J. E. , et al. 2017, AJ, 154, 207
Fischer, D. A., Marcy, G. W., & Spronck, J. F. P. 2014, ApJS, 210, 5
Fulton, B. J., Petigura, E. A., Howard, A. W., et al. 2017, AJ, 154, 109
Gaia Collaboration et al. 2016, A&A, 595, A2
Gaia Collaboration, Brown, A. G. A., Vallenari, A., et al. 2018, arXiv:1804.09365
Gillen, E., Hillenbrand, L. A., David, T. J., et al. 2017, ApJ, 849, 11
Hirano, T., Nowak, G., Kuzuhara, M. , et al. 2016, ApJ, 825, 53
Howell, S. B., Sobeck, C., Haas, M., et al. 2014, PASP, 126, 398
Huber, D., Bryson, S. T., Haas, M. R., et al. 2016, ApJS, 224, 2
Isaacson, H., & Fischer, D. 2010, ApJ, 725, 875
Lillo-Box, J., Demangeon, O., Santerne, A., et al. 2016, A&A, 594, A50
Lissauer, J. J., Marcy, G. W., Rowe, J. F., et al. 2012, ApJ, 750, 112
Mandel, K., & Agol, E. 2002, ApJL, 580, L171
Mann, A. W., Gaidos, E., Vanderburg, A., et al. 2017, AJ, 153, 64

Marigo, P., Girardi, L., Bressan, A., et al. 2008, A&A, 482, 883
Mayo, A. W., Vanderburg, A., Latham, D. W., et al. 2018, arXiv:1802.05277
Morton, T. D. 2015, Isochrones: Stellar Model Grid Package, Astrophysics Source Code Library, ascl:1503.010
Morton, T. D., Bryson, S. T., Coughlin, J. L., et al. 2016, ApJ, 822, 86
Oelkers, R. J., Rodriguez, J. E., Stassun, K. G., et al. 2018, AJ, 155, 39
Paletou, F., Böhm, T., Watson, V., & Trouilhet, J.-F. 2015, A&A, 573, A67
Parviainen, H., & Aigrain, S. 2015, MNRAS, 453, 3821
Petigura, E. A., Howard, A. W., & Marcy, G. W. 2013a, PNAS, 110, 19273
Petigura, E. A., Crossfield, I. J. M., Isaacson, H., et al. 2018, AJ, 155, 21
Petigura, E. A., Marcy, G. W., & Howard, A. W. 2013b, ApJ, 770, 69
Petigura, E. A., Schlieder, J. E., Crossfield, I. J. M. , et al. 2015, ApJ, 811, 102
Ricker, G. R., Winn, J. N., Vanderspek, R., et al. 2014, Proc. SPIE, 9143, 20
Santerne, A., Moutou, C., Tsantaki, M. , et al. 2016, A&A, 587, A64
Sinukoff, E., Howard, A. W., Petigura, E. A., et al. 2016, ApJ, 827, 78
Thompson, S. E., Coughlin, J. L., Hoffman, K., et al. 2018, arXiv:1710.06758
Valenti, J. A., & Fischer, D. A. 2005, ApJS, 159, 141
Vanderburg, A., & Johnson, J. A. 2014, PASP, 126, 948
Vanderburg, A., Latham, D. W., Buchhave, L. A., et al. 2016, ApJS, 222, 14
Wolfgang, A., Rogers, L. A., & Ford, E. B. 2016, ApJ, 825, 19